

HD 259440: THE PROPOSED OPTICAL COUNTERPART OF THE γ -RAY BINARY HESS J0632+057

CHRISTINA ARAGONA, M. VIRGINIA MCSWAIN

Department of Physics, Lehigh University, 16 Memorial Drive East, Bethlehem, PA 18015

MICHAËL DE BECKER

Institut d'Astrophysique et Géophysique, Université de Liège, B-4000 Liège, Belgium and
Observatoire de Haute-Provence, F-04870 Saint-Michel l'Observatoire, France

Accepted to ApJ

ABSTRACT

HD 259440 is a B0pe star that was proposed as the optical counterpart to the γ -ray source HESS J0632+057. Here we present optical spectra of HD 259440 acquired to investigate the stellar parameters, the properties of the Be star disk, and evidence of binarity in this system. Emission from the H α line shows evidence of a spiral density wave in the nearly edge-on disk. We find a best fit stellar effective temperature of 27500–30000 K and a log surface gravity of 3.75–4.0, although our fits are somewhat ambiguous due to scattered light from the circumstellar disk. We derive a mass of 13.2–19.0 M_{\odot} and a radius of 6.0–9.6 R_{\odot} . By fitting the spectral energy distribution, we find a distance between 1.1–1.7 kpc. We do not detect any significant radial velocity shifts in our data, ruling out orbital periods shorter than one month. If HD 259440 is a binary, it is likely a long period (> 100 d) system.

Subject headings: binaries: general – stars: emission-line, Be – stars: fundamental parameters – stars: individual (HD 259440, HESS J0632+057)

1. INTRODUCTION

HD 259440 (=MCW 443, BD +05 1291), which lies between the edge of the Monoceros Loop supernova remnant and the star forming region of the Rosette Nebula, is classified as a B0pe star by Morgan et al. (1955) and a BN0 mne star by Turner (1976). Gutiérrez-Soto et al. (2007) assign it a projected rotational velocity, $V \sin i$, of 430 km s⁻¹. Otherwise, no detailed optical study of this star has been performed. HD 259440 has been proposed as the optical counterpart to a possible new γ -ray binary, HESS J0632+057 (Aharonian et al. 2007). γ -ray binaries are a subset of high-mass X-ray binaries which also emit radiation in the MeV-TeV range. The very high energy emission in such objects is expected to originate from an interaction between the massive star's wind and the compact object, although the physical processes that produce this radiation are under debate (see e.g. Dubus 2006).

Observations taken with the HESS telescope array between 2004 March and 2006 March revealed the TeV point source HESS J0632+057 (Aharonian et al. 2007). Hinton et al. (2009) followed up this detection with a 26 ks observation of the field using *XMM-Newton* on 2007 September 17. XMMU J063259.3+054801, the brightest source in the field, was positionally coincident with the HESS observation and centered on HD 259440. The X-ray source showed a gradual decline in flux over the course of the observation. X-ray observations obtained with *Swift* showed flux variations on a variety of timescales, from several days to a month (Falcone et al. 2010). While the data did not show a clear periodicity, Falcone et al. (2010) determined that periods

of 35–40 days or ≥ 54 days are possibilities. HESS J0632+057 has also been associated with the *ROSAT* source 1RXS J063258.3+054857 and the EGRET source 3EG J0634+0521 (Aharonian et al. 2007; Skilton et al. 2009). The source has not yet been detected by *Fermi* (Abdo et al. 2010). A non-detection by VERITAS indicates a decrease in γ -ray flux from the time of the original HESS detection as well (Acciari et al. 2009). Radio observations revealed the source to have a mean flux of 0.3 mJy at 5 GHz, with variations on the timescale of a month (Skilton et al. 2009). The multiwavelength detections and the flux variations of this system are consistent with the class of γ -ray binaries.

Currently, six systems are known or proposed γ -ray binaries: LS 5039, LS I +61 303 (Abdo et al. 2010), PSR B1259–63 (Aharonian et al. 2005), Cyg X-1 (Albert et al. 2007), Cyg X-3 (Abdo et al. 2009), and HESS J0632+057 (see above). Optical spectroscopy can provide useful information about the stellar properties and orbital parameters of these systems, which aid in the analysis of observations at other wavelengths. We have undertaken a study of the optical properties of HD 259440 to complement ongoing work in X-ray, γ -ray, and radio to determine the nature of this system.

In order to determine the properties of HD 259440, we present an extensive collection of red and blue optical spectra. Section 2 describes our observations. Section 3 details our search for radial velocity variations and places limits on the orbital period for the system. We address the circumstellar disk features in Section 4. In Section 5, we discuss our fitting procedure using model spectra to determine the stellar properties. Section 6 describes the spectral energy distribution (SED) of the Be star. We summarize our results in Section 7.

2. OBSERVATIONS

We observed HD 259440 using the Kitt Peak National Observatory (KPNO) Coudé Feed (CF) telescope with the F3KB detector between 2008 October 17 and November 21. We used both blue and red spectral setups each night and generally obtained two spectra of HD 259440 in each. The blue spectra were taken using grating B in the third order with the 4-96 order sorting filter. They have a resolving power $R = \lambda/\Delta\lambda \sim 9500$, cover a wavelength range 4130 – 4570 Å, and have exposure times ranging from 20–30 minutes giving a signal-to-noise, S/N, of 50–140. The red spectra were obtained using grating B in the second order and the OG550 order sorting filter. They have $R \sim 12000$, span a wavelength range of 6400 – 7050 Å, and have exposure times of 20 minutes giving a S/N of 100–250. ThAr comparison lamp spectra were taken every 2–3 hours for wavelength calibrations. We zero corrected, flatfielded, and wavelength calibrated each spectrum using standard procedures in IRAF¹. All spectra were interpolated to a common wavelength grid and corrected for heliocentric radial velocity variations. The blue spectra were written to a common log wavelength scale for radial velocity analysis. The spectra were rectified in IRAF using emission line free continuum regions.

Two blue optical spectra were obtained at the KPNO 2.1m telescope using the GoldCam Spectrograph on 2008 December 12 – 13. Grating G47 was used in the second order with a CuSO₄ blocking filter and a slit width of 1.3" to achieve $R \sim 2100 - 3100$. These observations cover a wavelength range of 3700–4900 Å. The two spectra have exposure times of 15–20 minutes, resulting in a S/N of 125–150. Comparison spectra were taken using a HeNeAr lamp to wavelength calibrate the data. The spectra were zero corrected, flatfielded, and wavelength calibrated using the standard procedures in IRAF. We corrected the spectra for heliocentric radial velocity variations and rectified them in IRAF using emission line free continuum regions.

We also observed HD 259440 seven times, twice in 2009 March and five times in 2009 October, with the SOPHIE cross-dispersed échelle spectrograph at the Observatoire Haute-Provence (OHP) 1.93m telescope. These observations used the 52.65 l mm⁻¹ R2 échelle grating to cover 39 orders in the high efficiency mode ($R = 40000$) covering a wavelength range of 3872 – 6943 Å. The exposure times were between 45–90 minutes long, yielding a S/N of 80–220. Additional spectra were obtained from the OHP archive, which were taken between 2007 October and 2008 February. These spectra had shorter exposure times of 5–15 minutes, and S/N as low as 40. The spectra were corrected for blaze, flatfielded, wavelength calibrated using ThAr lamp spectra taken within 2 hours of each observation, and corrected for heliocentric radial velocity variations. The observations are summarized in Table 1.

3. CONSTRAINTS ON ORBITAL PERIOD

¹ IRAF is distributed by the National Optical Astronomy Observatory, which is operated by the Association of Universities for Research in Astronomy, Inc., under cooperative agreement with the National Science Foundation.

We performed a cross-correlation of the He I $\lambda 4471$ line in our CF data with a mean spectrum from that run to search for radial velocity, V_R , shifts. Due to the low S/N of those spectra, the V_R measurements had a standard deviation, σ_{RV} , of 20.1 km s⁻¹, and no significant shifts in V_R were found. We also did not detect any gradual trend of increasing or decreasing V_R . The CF dataset rules out orbital periods of ~ 35 d or less.

The He I $\lambda 5876$ line in the échelle spectra from OHP was also examined for V_R variations, of which the results are presented in Table 2. These measurements had a σ_{RV} of 6.7 km s⁻¹, which is close to the precision that we would expect to achieve due to the natural line width and line shape. Again, no significant shifts in V_R were detected in this set of observations. Due to the significant instrumental differences and wavelength coverage between the CF, KPNO 2.1m, and OHP runs, we hesitate to combine the V_R over these combined datasets to investigate V_R shifts. Crampton (1968) gives a radial velocity measurement of 7.6 km/s; however, the measurement is flagged for poor quality. Thus we use only the sparsely sampled OHP spectra to constrain the orbital period further.

We cannot rule out the possibility that HD 259440 is a binary until we determine the probability that the system has an orbit with V_R shifts too small for our observations to detect. We use a method similar to that outlined in Garmany et al. (1980). For a binary system, the mass function of the primary is

$$f(m) = \frac{M_\star \sin^3 i}{q(1+q)^2} = 1.0355 \times 10^{-7} K_\star^3 P (1-e^2)^{3/2} \quad (1)$$

with

$$q = \frac{M_\star}{M_X} \quad (2)$$

where M_\star is the mass of the optical star in solar units, M_X is the mass of the compact object in solar units, K_\star is the velocity semi-amplitude of the optical star in km s⁻¹, P is the orbital period in days, and e is the orbital eccentricity. Assuming an upper limit for K_\star of $2\sigma_{RV}$, we can find the upper limit for the system inclination for a given value of P at which we would fail to detect V_R variations in our dataset:

$$\sin i \leq 9.392 \times 10^{-3} \sigma_{RV} \left(\frac{Pq(1+q)^2(1-e^2)^{3/2}}{M_\star} \right)^{1/3} \quad (3)$$

If we assume a random distribution of orbital inclinations, the probability that V_R is lower than our detection limit is

$$P(i < i_{up}) = \int_0^{i_{up}} \sin i \, di = 1 - \cos i_{up}. \quad (4)$$

We used the lower σ_{RV} obtained from the OHP spectra and our measured mass of the Be star, $M_\star = 16 M_\odot$ (see Section 5). Secondary masses of 1.5, 2.0, and 2.5 M_\odot , consistent with a low mass companion, and eccentricities of 0.0, 0.2, 0.4, and 0.6 were considered. The results are plotted in Figure 1. For a compact companion of 1.5 M_\odot , we would be unable to detect V_R shifts for an orbital period greater than 50 days. The chance of detection improves for higher values of the secondary

mass. However, for a 100 day orbit, there is still only a 50% probability the the system will have an inclination favorable for detecting V_R shifts in our data. The chances of detection also decrease with orbital eccentricity. However, our method does not take into account that to detect the radial velocity shifts for an eccentric orbit, we would need to observe the system close to periastron. The system would only spend a small fraction of its orbit with V_R shifts high enough for us to detect, decreasing our chances of observing V_R shifts in systems of higher eccentricity. Therefore, we cannot rule out HD 259440 as a binary system with a long period.

4. CIRCUMSTELLAR DISK FEATURES

Our collection of red CF spectra provide an excellent tracer of the Be star’s disk emission over 35 nights. The mean equivalent width of the $H\alpha$ emission line, $W_{H\alpha}$, is -52.3 \AA , with a standard deviation of 0.7. We find that $W_{H\alpha}$ is constant within our estimated 2% error due to noise and the continuum placement. We show in Figure 2 the $H\alpha$ line profiles and a gray-scale image of this line over the span of the observing run. Since the orbital period of HD 259440 is unknown, neither the line profiles nor the gray-scale plots are folded by orbital phase, but rather they reveal true chronological variations in the line profile behavior as a function of heliocentric julian date (HJD).

We noticed some subtle temporal variations in the shape of the emission profile, so we subtracted the mean emission line profile to investigate the residuals more carefully. The $H\alpha$ emission residuals, and the corresponding gray-scales, are shown in Figure 3. These residual spectra reveal a partial S-shaped feature over the 35 nights of observation that suggest a characteristic period of ~ 60 days. We attribute these variations to a spiral density wave in the circumstellar disk, common among Be stars (Porter & Rivinius 2003).

The high $V \sin i$ for this star (see Section 5) implies that the disk inclination must be nearly 90° . Therefore we view the disk nearly edge-on. Since we do not resolve a double peaked profile in $H\alpha$, the disk is likely optically thick out to several stellar radii (consistent with the very high $W_{H\alpha}$). By contrast, $H\gamma$ shows a strong double-peaked emission profile. The disk also contributes a continuum flux to the line of sight which is added to the observed stellar spectrum, causing photospheric lines in the rectified spectra to appear too shallow. Bound-free emission will contribute a fraction of the stellar flux across all wavelengths, while free-free emission will increase at longer wavelengths. Indeed, we find evidence for such flux dilution in our blue spectra, discussed in the following section. We also observe an infrared excess in the SED for the system, which will be discussed in Section 6.

5. STELLAR PARAMETERS

Accurately determining the stellar parameters of HD 259440 is a challenging process due to the prevalence of emission features in the spectra. In order to minimize the impact of the disk emission on our analysis, we chose to focus on the He I and H Balmer lines with $\lambda \leq 4000 \text{ \AA}$, where the lines are predominantly in absorption. This approach required our analysis to use the lower resolution KPNO 2.1m telescope spectra, as these covered a broader

wavelength range than the KPNO CF data (Figure 4). In order to improve the S/N, we created a mean spectrum from the two observations. We then compared this spectrum to *Thusty* OSTAR2002 (Lanz & Hubeny 2003) and *BSTAR*2006 (Lanz & Hubeny 2007) model grids, corrected for instrumental broadening, to obtain values for the effective temperature, T_{eff} , surface gravity, $\log g$, and $V \sin i$ of the optical star.

The *Thusty* *BSTAR*2006 and OSTAR2002 model grids assume a plane-parallel stellar atmosphere. The *BSTAR*2006 models are available with temperatures ranging from 15000 K to 30000 K, with a grid spacing of 1000 K, and $\log g$ ranging from 1.75 to 4.75 where g is in cm s^{-2} , with a grid spacing of 0.25. The OSTAR2002 models exist for temperatures between 27500 K and 55000 K with a grid spacing of 2500 K. These models are available for $\log g$ between 3.0 and 4.75, with a grid spacing of 0.25. The OSTAR2002 models assume a microturbulence velocity of 10 km s^{-1} , while the *BSTAR*2006 models assume a microturbulence velocity of 2 km s^{-1} . We used models with solar abundances.

Initially, we tried fitting the mean spectrum of HD 259440 over the 3750–3950 \AA range for T_{eff} , $\log g$, and $V \sin i$ simultaneously. T_{eff} was varied between 20000 K and 40000 K in increments of 1000 K (2500 K) to match the spacing of the *BSTAR*2006 (OSTAR2002) grid. We varied $\log g$ from 2.50 to 4.75 (3.0 to 4.75) in increments of 0.25 according to the *BSTAR*2006 (OSTAR2002) grid spacings. We also increased $V \sin i$ from 300 km s^{-1} to 500 km s^{-1} in steps of 50 km s^{-1} . We computed the χ^2 value for each combination of T_{eff} , $\log g$, and $V \sin i$. However, none of the trials produced a satisfactory fit to the observed spectrum. The best fits from the two model grids produced divergent solutions for T_{eff} and $\log g$. Furthermore, a visual inspection comparing the model to the observed spectrum revealed the poor quality of these fits and they could not be used to constrain a T_{eff} and $\log g$ for the system.

The unusually shallow yet broad absorption lines seen in the spectra of HD 259440 are indicative of flux dilution, in that the continuum emission and scattering from the disk has effectively decreased the relative strength of absorption lines in the rectified spectra. The total observed flux is the sum of the flux from the disk, F_{disk} , and the star, F_{star} . Over a small wavelength range, we can assume a constant ratio $N = F_{\text{disk}}/F_{\text{star}}$. Using this assumption, we can correct for the disk continuum emission by adjusting the rectified spectrum:

$$F_{R,\text{star}} = F_R(1 + N) - N \quad (5)$$

where F_R is the rectified observed spectrum and $F_{R,\text{star}}$ is the rectified spectrum of the star corrected for the disk continuum emission. Since the relative disk flux is unknown, we adjusted the observed spectrum for values of $N = 0.1 - 0.9$ and repeated the fitting procedure at each value.

The absorption lines in the spectrum of HD 259440 are fairly broad, so we expect the star to have a high rotational velocity. At all values of T_{eff} and $\log g$, a $V \sin i$ of 500 km s^{-1} provided the best agreement with the line profiles. Therefore, we chose to fix $V \sin i$ at this value. We then repeated our fits using the OSTAR2002 and *BSTAR*2006 models over the 3750–3950 \AA region.

At each N , we determined the best fit T_{eff} and $\log g$ by minimizing the χ^2 from the model fits. Our quoted errors for T_{eff} and $\log g$ represent the 1σ significance levels from our best fit. For values of N between 0.0 and 0.4, T_{eff} and $\log g$ are not well constrained, but the fit quality and agreement between the BSTAR2006 and OSTAR2002 models improve significantly for higher values of N . Therefore, we chose to focus on the results with $N \geq 0.5$, which are summarized in columns 1–5 of Table 3.

A contour plot illustrating the 1σ , 2σ , and 3σ significance errors for the combined OSTAR2002 and BSTAR2006 model fits in the $N = 0.7$ case is shown in Figure 5. As can be seen from this figure and Table 3, the best values of T_{eff} for both the OSTAR2002 and BSTAR2006 models lie near the boundaries of the model grids. Furthermore, the 1σ significance contours are not closed at the boundary between the models. Therefore, we determined the lower limit of T_{eff} from the 1σ contour of the BSTAR2006 models and the upper limit from the 1σ contour of the OSTAR2002 models.

A *TruSty* BSTAR2006 model spectrum with $T_{\text{eff}} = 30000$ K, $\log g = 4.0$, and $V \sin i = 500$ km s $^{-1}$ plotted against the mean spectrum of HD 259440 with $N = 0.7$ is shown in Figure 6. We generally find good agreement between the model and observed spectrum in the H Balmer lines, although the He I $\lambda 3819$ line appears stronger than all of our model fits. HD 259440 has been classified as a star with peculiar abundances. It was marked as nitrogen rich by Turner (1976) and may also be a helium-strong star. We cannot distinguish significant differences between the model fits with different values of N , hence some ambiguity in the physical parameters of this system.

As a further test of the validity of the fit, we compared the model fits to one of the few other photospheric absorption lines in our blue spectra, the flux-corrected He I $\lambda 4471$ line. Figure 7 shows good agreement over the core of the line with the BSTAR2006 fit and $N = 0.7$. There may be some excess emission in the line wings from the higher velocity regions of the disk, narrowing the line slightly. Using the OSTAR2002 fits, the flux-corrected He I $\lambda 4471$ line is again stronger than the model, a result of the difference in microturbulent velocity between the two sets of models. Since HD 259440 may be He strong, the fit of the He I $\lambda 4471$ line does not help constrain the best fit any further. The quality of the fits for the values of N considered in this paper were equally good, so we also cannot constrain the flux contribution from the disk any further.

We determined the mass, M_* , and radius, R_* , of the star using our best fit values for T_{eff} and $\log g$ and interpolating between the evolutionary tracks of Schaller et al. (1992). The evolutionary tracks were published for non-rotating stars with solar metallicity and masses ranging from 0.8 to 120 M_{\odot} . The errors for M_* were calculated using the best value of $\log g$ and using the 1σ limits for T_{eff} , while the errors for R_* were calculated using the best fit values for T_{eff} and using the 1σ limits for $\log g$. Our measurements of M_* and R_* are presented in columns 6–9 of Table 3. The rapid rotation of HD 259440 may result in an underestimation of the mass and introduce an additional systematic error into our measurements. Ekström et al. (2008) calculated evolutionary tracks for

rapidly rotating stars. Comparing these models to the tracks from Schaller et al. (1992), we conclude that any discrepancy in the mass of HD 259440 would be about 5 M_{\odot} . We also calculated the critical velocity, V_{crit} , at the stellar equator for each N . Since HD 259440 is a rapid rotator, the stellar radius at the equator is $1.5R_*$ in the standard Roche model. Therefore,

$$V_{\text{crit}} = \sqrt{\frac{GM_*}{1.5R_*}}. \quad (6)$$

The results are listed in column 10 of Table 3. These results indicate that HD 259440 is rotating close to V_{crit} , which is plausible for Be stars and thought to contribute to the formation of the circumstellar disk (Townsend et al. 2004).

6. SPECTRAL ENERGY DISTRIBUTION

We compared the observed SED of HD 259440 with the model SEDs from the *TruSty* BSTAR2006 and OSTAR2002 models to measure the distance to the star. We obtained ultraviolet broadband photometric fluxes from Wesseliuss et al. (1982), Johnson *UBV* magnitudes from Neckel & Chini (1980), Johnson *I* magnitude from Droege et al. (2007), 2MASS *JHK_S* magnitudes from Skrutskie et al. (2006), and mid-infrared fluxes from Egan et al. (2003). The Johnson magnitudes were converted to fluxes according to Bessel et al. (1998), while the 2MASS photometry were converted to fluxes using Cohen et al. (2003).

The *TruSty* model spectra were binned in 50 Å bins to eliminate small scale line features and simplify comparison with the observed fluxes. A reddening of $E(B-V) = 0.85$ (Friedemann 1992) and selective extinction of $R = 3.1$ were applied to the model SEDs using the extinction model of Fitzpatrick (1999). The observed photometric fluxes were corrected for disk emission using each value of N and compared with the best fit OSTAR2002 and BSTAR2006 models.

In our spectral fitting, we assumed that the disk flux ratio N is constant over a small wavelength range. Therefore, we compared the observed fluxes between 3000 – 5000 Å, corrected for N , to the model SEDs to determine the angular diameter, θ_R :

$$\theta_R = \frac{R_*}{d} = \sqrt{\frac{F_{*,\text{obs}}}{F_{*,\text{surf}}}} = \sqrt{\frac{F_{\text{tot,obs}}}{F_{*,\text{surf}}(1+N)}} \quad (7)$$

where $F_{*,\text{obs}}$ is the observed flux produced by the star, $F_{*,\text{surf}}$ is the flux at the stellar surface, $F_{\text{tot,obs}}$ is the combined flux of the star and disk, and d is the distance to the star. Using our derived R_* with the calculated θ_R , we find that HD 259440 lies within the distance range $d = 1.1 - 1.7$ kpc. The errors in the distance presented in Table 3 give the standard deviation between the model SED and the broadband photometric flux points in the 3000 – 5000 Å range. As the quality of all our best fits were similar for values of N between 0.5 and 0.9, the actual error in d is more accurately reflected by the range of values presented. HD 259440 is listed by Voroshilov et al. (1985) as a member of the open cluster NGC 2244. A recent study by Bonatto & Bica (2009) places the cluster at 1.6 ± 0.2 kpc from the Sun, a value consistent with previous studies and our measurements for HD 259440

(Ogura & Ishida 1981; Pérez et al. 1987; Park & Sung 2002).

We expect to see exorbitant infrared emission in the SED of HD 259440 due to the nearly edge-on circumstellar disk. This infrared excess can clearly be seen in Figure 8, which shows the observed broadband photometric fluxes with the BSTAR2006 model SED for $T_{\text{eff}} = 30000$ K, $\log g = 4.0$, $N = 0.7$, and $d = 1.30$ kpc. At blue optical wavelengths, the disk contributes $\sim 0.7F_{\star}$. In the mid-infrared, the disk continuum emission is ~ 22 times the flux of the star.

7. SUMMARY OF RESULTS

HD 259440 is a main sequence B0pe star that may be helium strong. Due to continuum emission and scattered light from the disk contaminating the stellar spectrum, our measurements of its physical parameters are somewhat ambiguous. We find $T_{\text{eff}} \approx 30000$ K and $\log g \approx 4.0$. From the evolutionary tracks of Schaller et al. (1992), our best model fits indicate that the star has a mass of about $16 M_{\odot}$ and radius of about $6.6 R_{\odot}$. We find an angular radius of $23.5\text{--}25.7 \mu\text{as}$ and a distance range of $1.1\text{--}1.7$ kpc. Due to the non-detection of radial velocity shifts over our 35 nights of CF data, we can rule out the possible 35–40 d orbital period suggested by Falcone et al. (2010). However, longer period orbits would produce V_R shifts that would be lost in the noise of our data sets. Therefore, we cannot rule out HD 259440 as a binary with a period greater than 100 days, which would be consistent with the class of non-accreting X-ray binaries.

We would like to thank Wenjin Huang for allowing us to obtain spectra of HD 259440 during his KPNO 2.1m telescope time in December 2008. We also thank Yves Gallant, Bertrand Plez, and Guillaume Dubus, whose observations comprise the OHP archival spectra used in this paper. Also, we appreciate helpful conversations with Marc Gagné, Stan Owocki, Guillaume Dubus, and Doug Gies about this work. We are grateful for support from NASA DPR numbers NNX08AV70G, NNG08E1671, and NNX09AT67G. MVM is grateful for an institutional grant from Lehigh University. This publication makes use of data products from the Two Micron All Sky Survey, which is a joint project of the University of Massachusetts and the Infrared Processing and Analysis Center/California Institute of Technology, funded by the National Aeronautics and Space Administration and the National Science Foundation.

Facilities: KPNO:2.1m (), KPNO:CFT (), OHP:1.93m ()

REFERENCES

- Abdo, A. A., et al. 2009, *Science*, 326, 1512
 Abdo, A. A., et al. 2010, *ApJS*, 188, 405
 Acciari, V. A., et al. 2009, *ApJ*, 698, 94
 Aharonian, F., et al. 2005, *A&A*, 442, 1
 Aharonian, F. A., et al. 2007, *A&A*, 469, L1
 Albert, J., et al. 2007, *ApJ*, 665, L51
 Bessell, M. S., Castelli, F., & Plez, B. 1998, *A&A*, 333, 321
 Bonatto, C., & Bica, E. 2009, *MNRAS*, 394, 2127
 Cohen, M., Wheaton, Wm. A., & Megeath, S. T. 2003, *AJ*, 126, 1090
 Crampton, D. 1968, *AJ*, 73, 338
 Droege, T. F., Richmond, M. W., & Sallman, M. 2007, *PASP*, 119, 1083
 Dubus, G. 2006, *A&A*, 456, 801
 Egan, M. P., et al. 2003, *The Midcourse Space Experiment Point Source Catalog Version 2.3*
 Ekström, S., Meynet, G., Maeder, A., & Barblan, F. 2008, *A&A*, 478, 467
 Falcone, A. D., Grube, J., Hinton, J., Holder, J., Maier, G., Mukherjee, R., Skilton, J., & Stroh, M. 2010, *ApJ*, 708, L52
 Fitzpatrick, E. 1999, *PASP*, 111, 63
 Friedemann C. 1992, *CDS Inf. Bull.*, 40, 31
 Garmany, C. D., Conti, P. S., & Massey, P. 1980, *ApJ*, 242, 1063
 Gutiérrez-Soto, J., Fabregat, J., Suso, J., Lanzara, M., Garrido, R., Hubert, A.-M., & Floquet, M. 2007, *A&A*, 476, 927
 Hinton, J. A., et al. 2009, *ApJ*, 690, L101
 Lanz, T., & Hubeny, I. 2003, *ApJS*, 146, 417
 Lanz, T., & Hubeny, I. 2007, *ApJS*, 169, 83
 Morgan, W. W., Code, A. D., & Whitford, A. E. 1955, *ApJS*, 2, 41
 Neckel, T., & Chini, R. 1980, *A&AS*, 39, 411
 Ogura, K., & Ishida, K. 1981, *PASJ*, 33, 149
 Park, B., & Sung, H. 2002, *AJ*, 123, 892
 Pérez, M. R., Thé, P. S., & Westerlund, B. E. 1987, *PASP*, 99, 1050
 Porter, J. M., & Rivinius, T. 2003, *PASP*, 115, 1153
 Schaller, G., Schaerer, D., Meynet, G., & Maeder, A. 1992, *A&AS*, 96, 269
 Skilton, J. L., et al. 2009, *MNRAS*, 399, 317
 Skrutskie, M. F., et al. 2006, *AJ*, 131, 1163
 Townsend, R. H. D., Owocki, S. P., & Howarth, I. D. 2004, *MNRAS*, 350, 189
 Turner, D. G. 1976, *ApJ*, 210, 65
 Voroshilov, V. I., Guseva, N. G., Kalandadze, N. B., Kolesnik, L. N., Kuznetsov, V. I., Metreveli, M. D., & Shapovalov, A. N. 1985, *Catalogue of BV magnitudes and spectral classes for 6000 stars* (Kiev, Ukraine: Ukrainian Acad. Nauk)
 Wesselius, P. R., van Duinen, R. J., de Jonge, A. R. W., Aalders, J. W. G., Luinge, W., Wildeman, K. J. 1982, *A&AS*, 49, 427

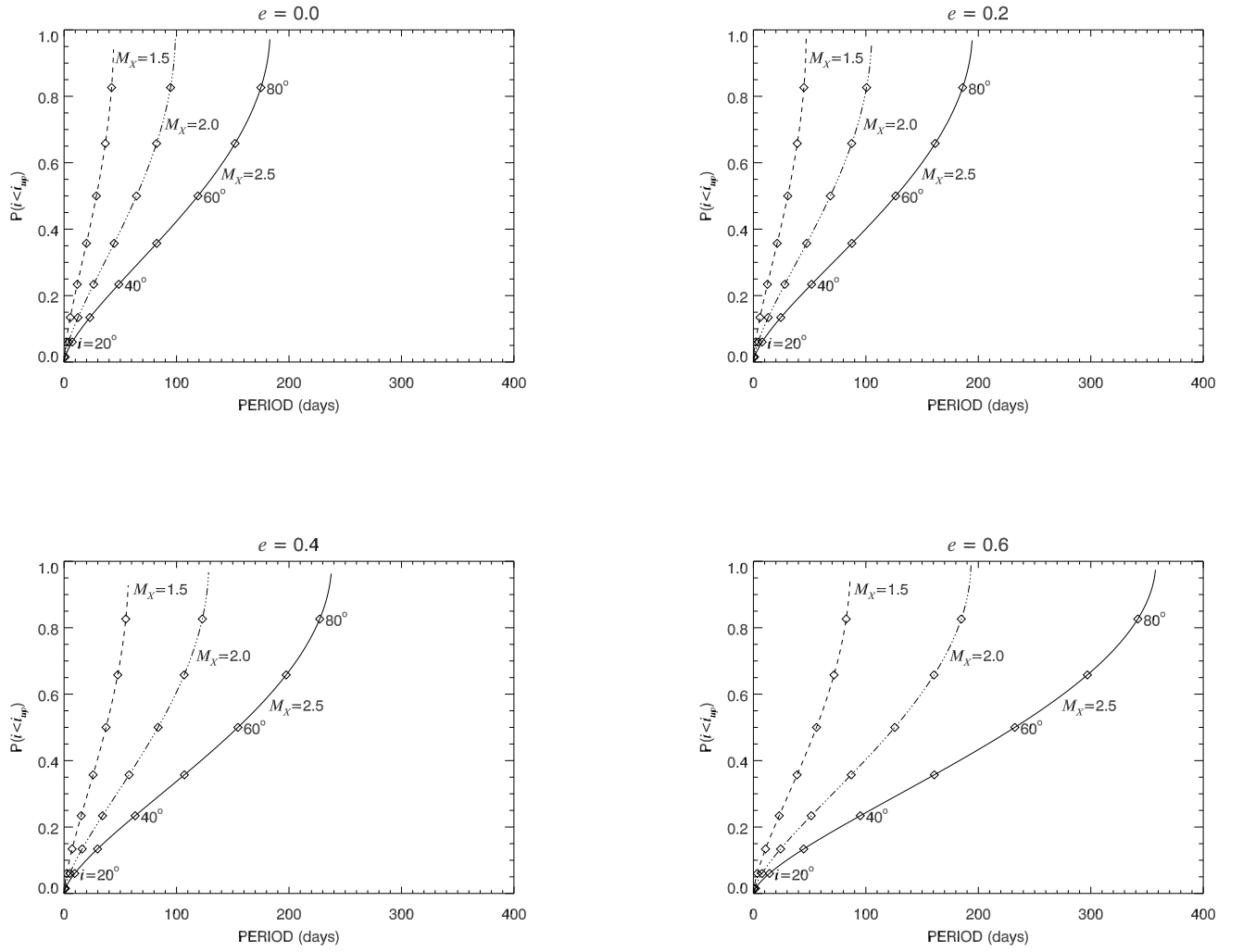


Figure 1. Probability to have missed the binary companion because of a too low inclination angle as a function of the orbital period, for eccentricities equal to 0.0, 0.2, 0.4, and 0.6, respectively. In each panel, three different secondary masses have been assumed. The diamonds indicate inclinations from 10° to 80° , spaced at intervals of 10° .

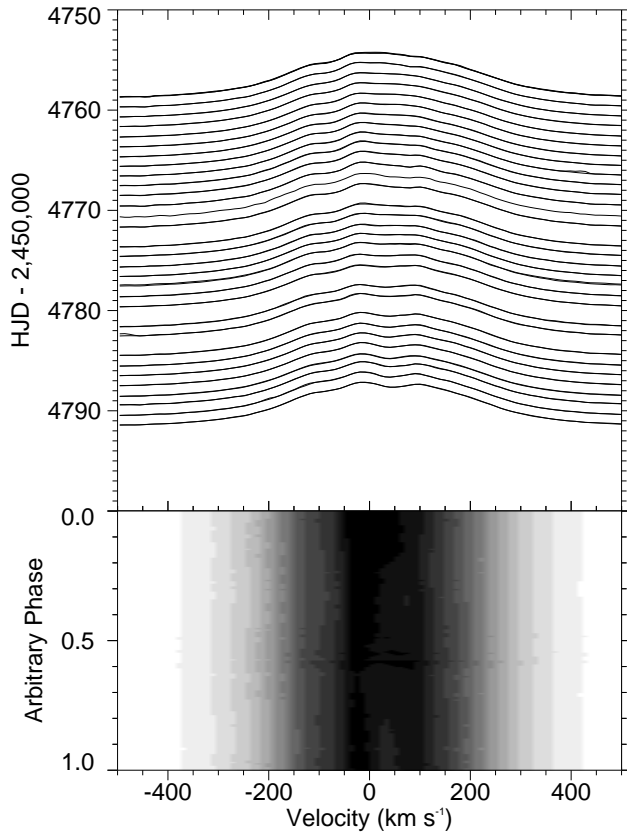


Figure 2. The upper plot shows the H α line profile of HD 259440 over our continuous 35 nights of observation with the CF, sorted by HJD, and the lower plot shows a gray-scale image of the same line. Since no period is currently known, the “Arbitrary Phase” goes from 0 at the start of the observing run to 1.0 at the end of the run. The intensity at each velocity in the gray-scale image is assigned one of 16 gray levels based on its value between the minimum (bright) and maximum (dark) observed values. The intensity between observed spectra is calculated by a linear interpolation between the closest observed phases.

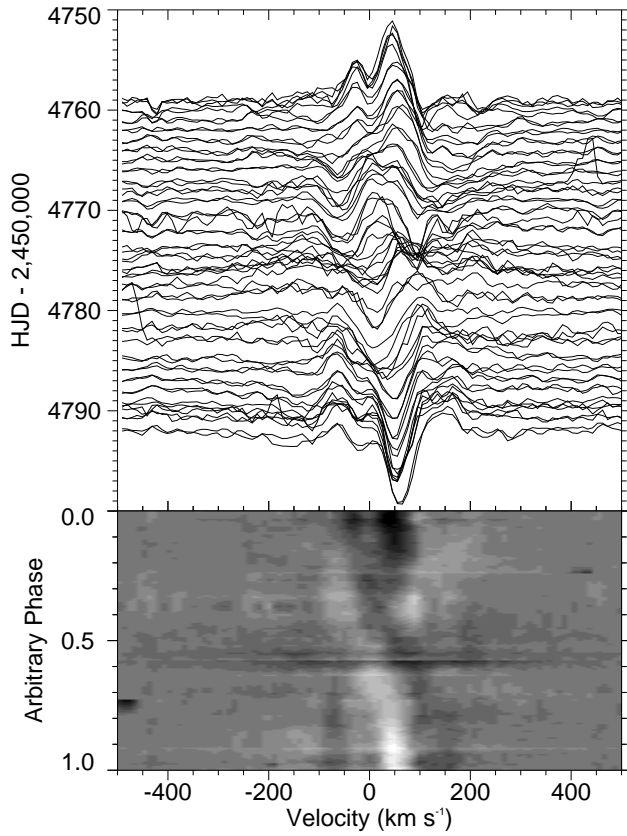


Figure 3. The upper panel shows the H α residual spectra of HD 259440, and the bottom panel shows a grayscale plot of the same residuals, in the same format as Fig. 2. The residual spectra reveal variations in the H α line with a ~ 60 d period that we attribute to a spiral density wave in the circumstellar disk.

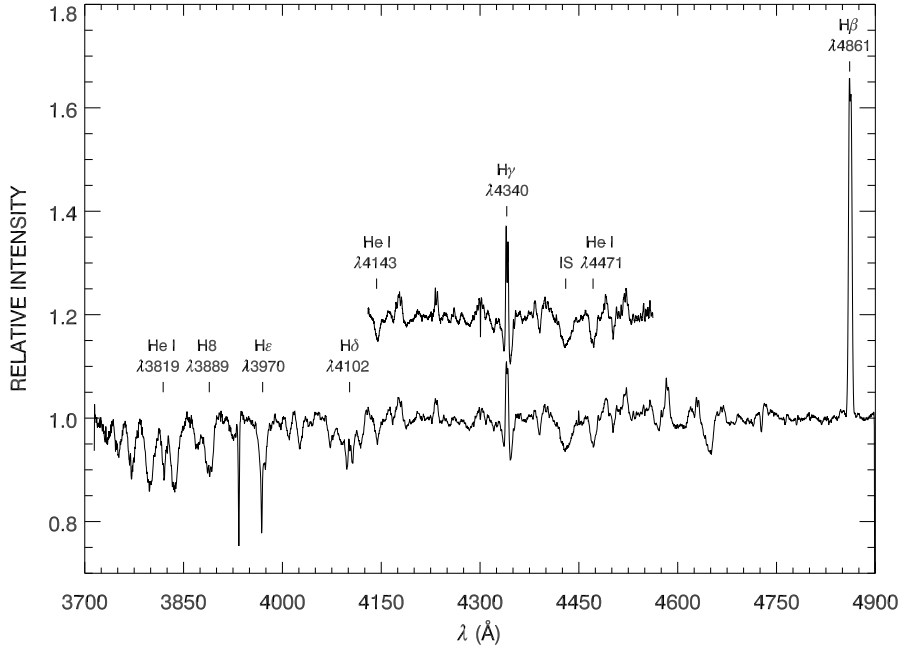


Figure 4. The mean spectra from the KPNO 2.1m (bottom) and CF (top) telescopes are plotted for comparison. The CF spectrum is offset by 0.2 for clarity.

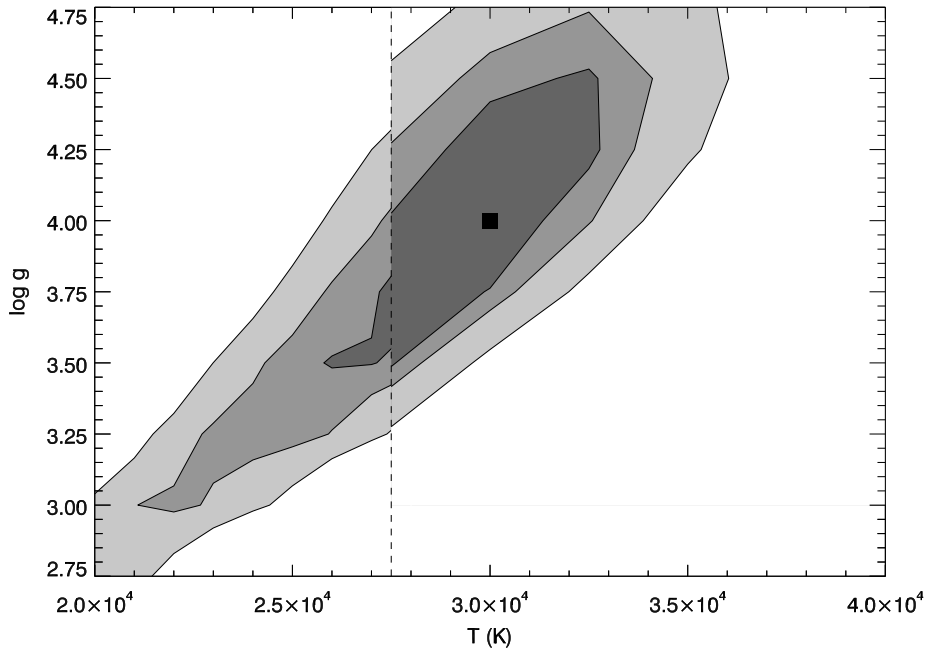


Figure 5. A contour plot of the 1σ , 2σ , and 3σ errors from the spectral fits using $N = 0.7$ and $V \sin i = 500 \text{ km s}^{-1}$. The discontinuity between the OSTAR2002 and BSTAR2006 models is marked by the vertical dashed line. The square represents the model with the lowest χ^2 value for both model fits.

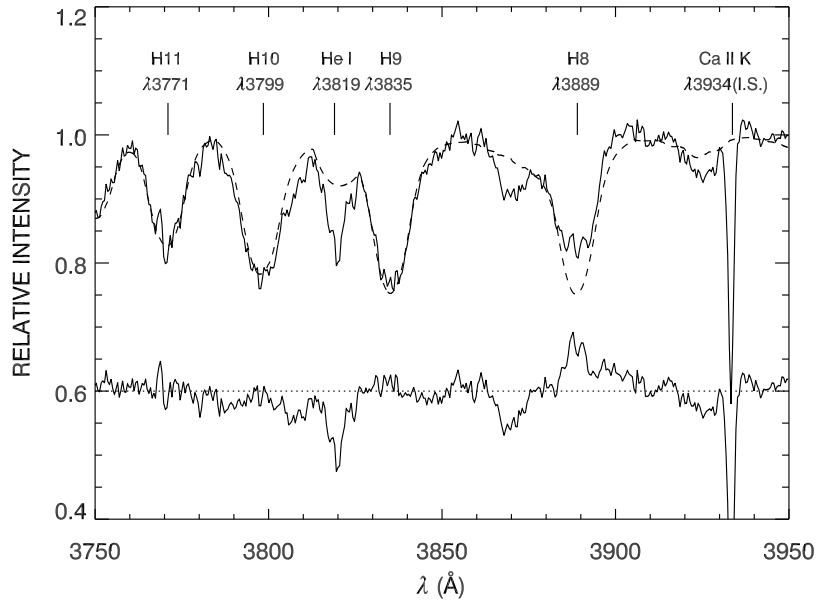


Figure 6. The mean KPNO 2.1m spectrum, adjusted for $N = 0.7$, is shown as a solid line. The dashed line shows the Tlustý BSTAR2006 model spectrum with $T_{\text{eff}} = 30000$ K, $\log g = 4.0$, and $V \sin i = 500$ km s $^{-1}$. The residuals from the fit are plotted below the spectrum, shifted by 0.6 for easier comparison.

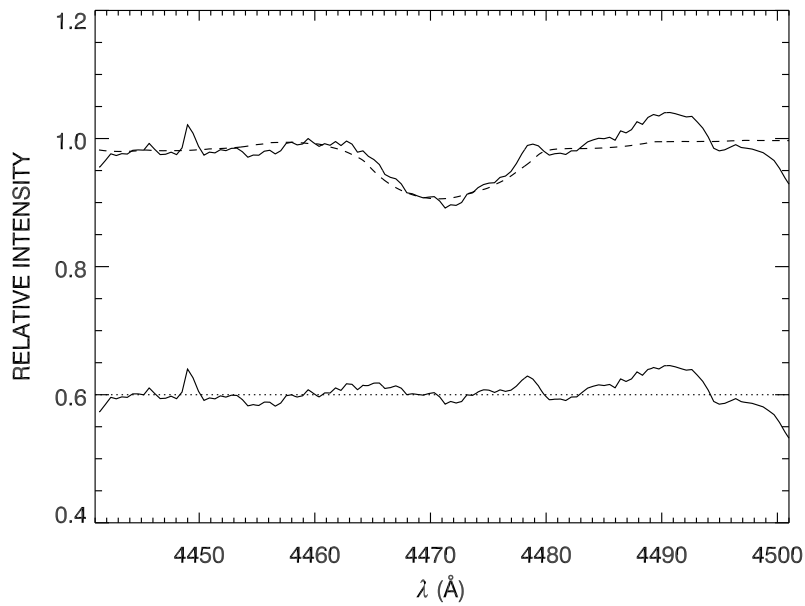


Figure 7. The He I $\lambda 4471$ line from the mean KPNO 2.1m spectrum is shown in the same format as Figure 6.

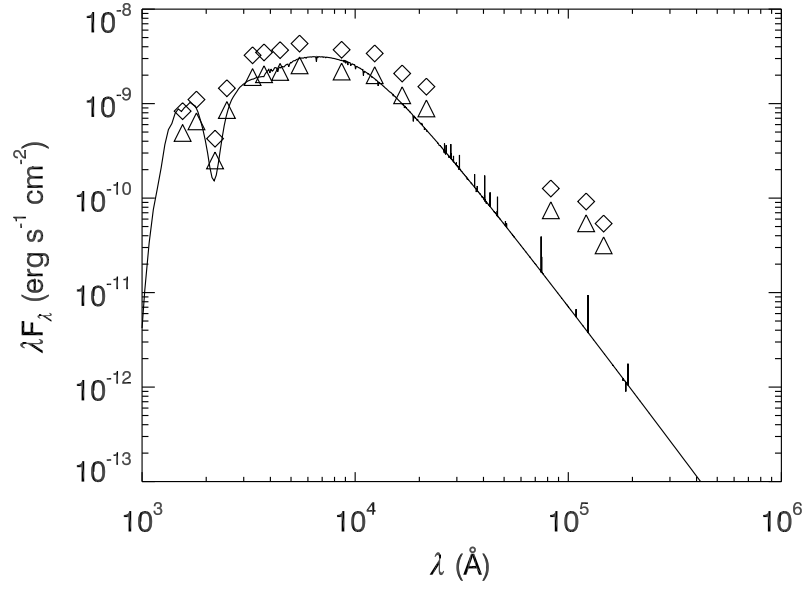


Figure 8. The Tlusty BSTAR2006 model SED normalized to $\theta_R = 24.3 \mu\text{as}$ is plotted as a solid line. The diamonds indicate the observed broadband photometric fluxes. The triangles represent the estimated stellar flux assuming $N = 0.7$.

Table 1
Journal of Spectroscopy

UT Dates	Telescope	λ Range (Å)	Resolving Power ($\lambda/\Delta\lambda$)	Grating/ Order	Filter	Number of Spectra
2007 Oct–2008 Feb	OHP 1.93m	3872 – 6943	40000	R2/50–88	...	16
2008 Oct 17–Nov 21	KPNO CF	4130 – 4570	9500	B/3	4-96	68
2008 Oct 17–Nov 21	KPNO CF	6400 – 7050	12000	B/2	OG550	62
2008 Dec 12–13	KPNO 2.1m	3700 – 4900	2100–3100	G47/2	CuSO ₄	2
2009 Mar	OHP 1.93m	3872 – 6943	40000	R2/50–88	...	2
2009 Oct	OHP 1.93m	3872 – 6943	40000	R2/50–88	...	5

Table 2
OHP V_R Measurements

UT Date	Mid-exposure HJD–2450000	V_R km s ⁻¹
2007 Oct 02	4375.1714	43.78
2007 Oct 22	4395.1686	47.55
2007 Oct 22	4395.1744	46.69
2007 Nov 01	4405.1763	47.96
2007 Nov 02	4406.1672	46.48
2007 Nov 03	4407.1905	44.90
2007 Nov 04	4408.1886	47.04
2007 Nov 05	4409.1474	41.74
2007 Nov 10	4414.0348	47.81
2007 Dec 27	4461.9402	41.99
2007 Jan 19	4484.8059	38.06
2008 Jan 21	4486.8267	28.88
2008 Feb 06	4502.9462	30.41
2008 Feb 12	4508.8925	36.28
2008 Feb 19	4515.8693	31.02
2008 Feb 25	4521.8527	27.09
2009 Mar 10	4900.8138	33.11
2009 Mar 14	4904.7721	45.97
2009 Oct 13	5117.6426	39.85
2009 Oct 15	5119.6701	43.57
2009 Oct 17	5121.6604	41.69
2009 Oct 27	5131.6605	42.96
2009 Oct 28	5132.6867	47.04

Table 3
Stellar Parameters

N	T_{eff} (K)	ΔT_{eff} (K)	$\log g$ (dex)	$\Delta \log g$ (dex)	M_* (M_{\odot})	ΔM_* (M_{\odot})	R_* (R_{\odot})	ΔR_* (R_{\odot})	V_{crit} (km s ⁻¹)	θ_D (μas)	$\Delta \theta_D$ (μas)	d (kpc)	Δd (kpc)
BSTAR2006 Model Fitting Results													
0.5	30,000	+1,000 -7,000	3.75	+0.90 -0.85	19.0	+1.5 -8.2	9.6	+44.8 -6.9	501	25.1	±1.1	1.78	±0.08
0.6	29,000	+4,000 -3,000	3.75	+0.80 -0.30	17.6	+6.7 -4.0	9.3	+5.9 -6.4	491	25.2	±1.2	1.71	±0.09
0.7	30,000	+3,000 -5,000	4.00	+0.50 -0.50	16.0	+3.6 -5.0	6.6	+8.1 -3.3	555	23.7	±1.1	1.30	±0.06
0.8	30,000	+2,000 -5,000	4.00	+0.50 -0.55	16.0	+2.5 -5.0	6.6	+9.7 -3.3	555	23.1	±1.1	1.33	±0.06
0.9	29,000	+2,000 -6,000	4.00	+0.45 -0.60	14.5	+2.9 -5.3	6.3	+7.7 -2.9	541	23.4	±1.2	1.26	±0.07
OSTAR2002 Model Fitting Results													
0.5	30,000	+1,000 -7,000	4.00	+0.65 -1.10	16.0	+1.4 -6.8	6.6	+47.8 -3.9	555	24.5	±1.0	1.25	±0.05
0.6	30,000	+3,000 -4,000	4.00	+0.55 -0.55	16.0	+3.6 -4.4	6.6	+9.7 -3.5	555	23.7	±0.9	1.30	±0.05
0.7	30,000	+3,000 -5,000	4.00	+0.50 -0.50	16.0	+3.6 -5.0	6.6	+8.1 -3.3	555	23.0	±0.9	1.34	±0.05
0.8	27,500	+4,500 -2,500	3.75	+0.60 -0.30	15.3	+7.2 -2.8	8.6	+5.5 -5.6	476	24.5	±1.2	1.64	±0.08
0.9	27,500	+3,500 -4,500	4.00	+0.45 -0.60	13.2	+4.2 -4.0	6.0	+9.4 -2.8	529	24.1	±1.3	1.16	±0.06

Note. — The errors in T_{eff} and $\log g$ were calculated using the OSTAR2002 results to determine the upper limits and the BSTAR2006 results to determine the lower limits.